FATIGUE FRACTURE MECHANICS OF LASER PBF TITANIUM ALLOY

A. Kasami[1], S. Maruta[1], S. Suzukake[1], Y.Imai[1] and H. Ishikawa[1]

[1] *Research and Innovation centre, Mitsubishi Heavy Industries, Ltd.
akiko.kasami.fy@mhi.com

Abstract: Additive Manufacturing (AM) is expected to enable weight reduction, cost saving as well as time reduction due to high freedom of design. Fatigue properties of AM Ti-6Al-4V by laser powder bed fusion (PBF) is relevant to its process parameters. In order to control the fatigue properties of Ti-6Al-4V ELI manufactured by selective laser PBF, fracture mechanism was investigated by fatigue tests and fatigue life cycle prediction. Fatigue samples were prepared with different build parameters and post process, which include heat treatment, HIP and machining. It was revealed the surface defects or internal defects were observed at the fatigue crack initiation sites. With the dimensional feature of these defects at the fatigue crack initiation sites, fatigue crack propagation cycles were calculated and compared with the experimental results.

Keywords: Additive Manufacturing, AM, Ti-6Al-4V, Fatigue life prediction

BACKGROUND

Additive Manufacturing (AM) has a high degree of design freedom to aero structural parts with complex shapes and it brings superior performance at the level of which was unable by conventional processes. While Ti alloys by AM is expected to bring significant weight reduction as well as time and cost saving in aerospace components, structural components of aerospace application have severe requirements for fatigue property control. Since the mechanical properties of metallic materials produced by AM vary greatly depending on the powder used as the raw material and the process parameters, it is important to control the three major parameters which governs the fatigue properties in order to satisfy with high reliability and reproducibility; surface topography, internal defects and microstructures that govern the fatigue properties of AM parts. Therefore, the purpose of this study is to quantitatively grasp the effect of internal defects and microstructure through experiments and analysis using linear fracture mechanics in order to clarify the effect of manufacturing process on the fatigue properties of Ti -6 Al -4 V alloy produced by laser powder bed fusion (PBF).

EXPERIMENTAL PROCEDURE

Samples

Table 1 shows the powder, deposition parameters, heat treatment conditions and surface finish of the test samples. Table 2 shows the matrix of specimens. To compare the differences in internal defects and surface roughness, the specimens shown in Fig. 1 were prepared under different conditions of build parameters, heat treatment and surface finish. In order to compare the effect of the difference in

surface condition between As-built and Machined, two types of surface finishes were produced with or without machining after deposition.

Table 1 Deposition parameters and post process conditions.

Powder	Ti-6Al-4V ELI(15-45μm, AP&C)
Machine	EOS M290
Build direction	Z (Load direction is parallel to build direction)
Heat treatment	Anneal: 900℃, 2hr in vacuum furnace HIP: 900℃, 2hr
Surface finish	As-built or machined

Table 2 Test matrix.

ID	Build parameter	Heat treatment	Surface finish	Description
M/C	Standard	Anneal	Machined	Baseline (Medium defects)
LowE-M/C	Low energy	Anneal	Machined	Many defects
HIP-M/C	Standard	HIP	Machined	Less defects
As-built	Standard	Anneal	As-built	Baseline (Medium defects)
HIP-As-built	Standard	HIP	As-built	Small defects

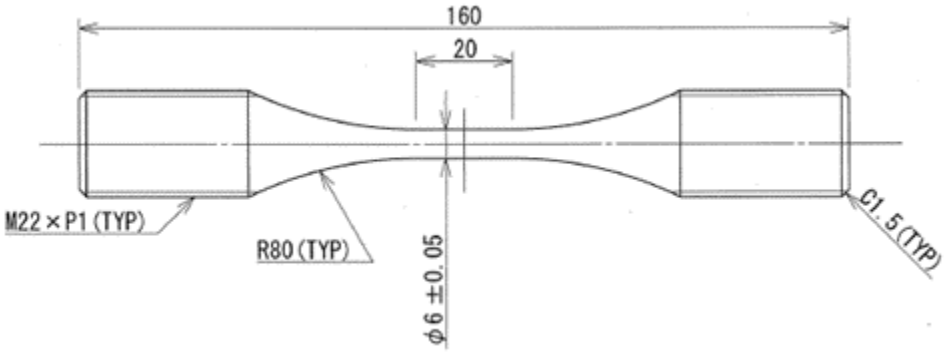

Fig.1 Fatigue test specimen

Fatigue test

Fatigue tests were carried out in a uniaxial tensile fatigue test (R = 0.1) in a room-temperature environment under load control at the frequency of 5 ~ 15 Hz. The stress level of the fatigue fracture life at 2.0×10^6 and/or more is defined as run-out, which means the apparent fatigue limit.

RESULTS

Fatigue test results

Figure 2 shows the S-N curves of the fatigue test results. The vertical axis is stress amplitude of arbitrary unit, which was derived by dividing the maximum stress amplitude of all the tests performed.

Comparing the three conditions with machining, the S-N curve tended to shift to the upper right in the order of Low Energy + Machined (LowE-M/C), M/C, and HIP + Machined (HIP-M/C). In particular, the fatigue strength at long life cycles tends to decrease significantly, and the fatigue limit of HIP-M/C was nearly twice that of LowE-M/C. The S-N curves of Baseline-as-built (As-built) and as-built with HIP (HIP-As built) were lower in fatigue strength than those of HIP-M/C, M/C and LowE-M/C. The fatigue limit of Baseline-As-built (As-built) was about half that of LowE-M/C, and

no significant difference in fatigue limit was observed between with or without HIP as long as its surface is not modified.

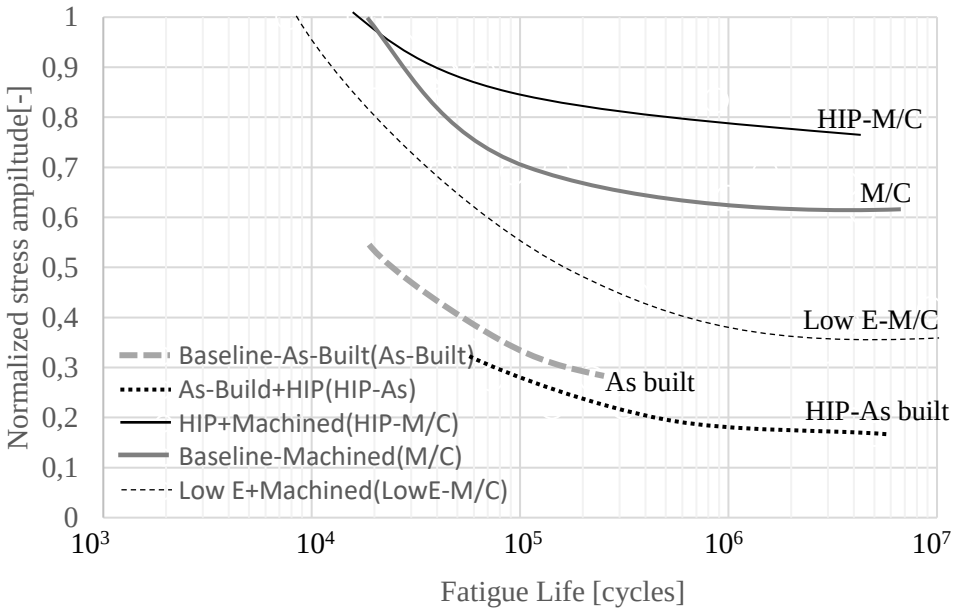

Fig.2 S-N Curves of laser PBF Ti-Al-4V.

Fatigue fracture analysis

Fracture surface observation on the fractured specimens was performed by SEM. Figure 3 shows typical photographs of the observations. Figure 3(a) and (b) are fracture surface photographs of the machined specimen, Figure 3(a) of the HIP-M/C specimen and Figure 3(b) of the LowE-M/C specimen. Both of them show that fatigue crack initiates at the single location on surface. The difference between Figure 3(a) and (b) is that although all of them showed crack growth from the fatigue crack initiation site of the surface, (a) showed no obvious evidence at the fatigue crack initiation site, while (b) showed a defect of about 100 microns in width near the fatigue crack initiation site. The defect observed at the fatigue crack initiation site of (b) is presumed to be a lack of fusion from its geometric features.

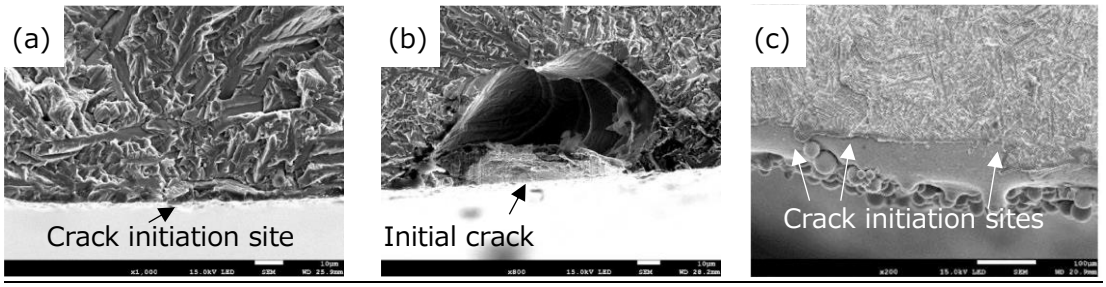

Fig. 3 Fatigue fracture surfaces. (a) HIP+Machined(HIP-M/C), (b) Low energy + Machined (LowE-M/C) and (c) Baseline- As-built(As-buit). Arrows in the pictures indicates crack initiation sites.

Figure 3(c) is a SEM image of fracture surface in As-built specimen. Like the other two, this was also a surface initiation and a multi-site crack where cracks propagate from several locations on the surface. In addition, for As-built specimens, there was no significant difference in the appearance of the crack initiation site whether it was HIPed or not.

Cross sectional observation

Cross-sectional observations of typical samples were performed on three types of machined specimens to confirm the occurrence of internal defects. Figure 4 shows the optical microscopic images.
In HIP-M/C, few defects were observed by optical microscopy, while in M/C and LowE-M/C, several defects of 10 ~ 100 μm in cross section were observed. In addition, more defects were found in LowE-M/C than in M/C, and they tended to be larger in size.

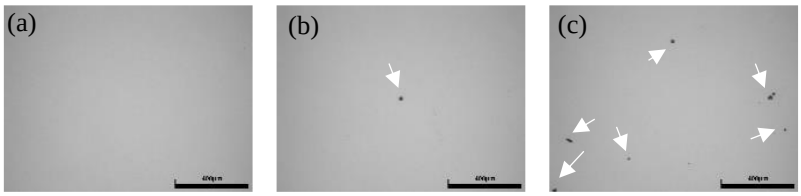

Fig. 4 Optical microscopic observations of (a) HIP+Machined(HIP-M/C), (b) Baseline-Machined(M/C) and (c) Low energy + Machined(LowE-M/C). Arrows indicate internal defects.

DISCUSSION

Fatigue life prediction

From the results of the fracture surface observation, no significant difference was found between the different build conditions and post process. This suggests that the difference in fatigue life cycle is not caused by the microstructure but by defects. Therefore, in order to evaluate the effect of defects on fatigue strength, the crack propagation cycles were estimated based on the shape and size of defects at the fatigue crack initiation site obtained from the fracture surface observation results, and the life of each specimen was estimated.

Estimation of initial crack size

From the fracture surface observation results, when a defect was observed at the fatigue crack initiation site, the size of the defect was regarded as the initial crack size, and the initial crack was estimated by converting the shape of the defect to the initial crack size of √area. The estimation was based on the geometrical characteristics of the defects (Figure 5) and was approximated under the following three conditions.

(1) Surface defects with the ratio of crack depth c to width 2a is more than 10, (2a/c < 10, Fig.5(1))
The square root of the projected area of the defect observed at the fatigue crack initiation site was derived as the initial defect dimension √area.

(2) Surface defects with the ratio of crack depth c to width 2a, (2a/c ≧ 10, Figure 5(2))
In the case of a shape with defects opening widely to the surface, the initial crack size √area is estimated as √area = √10×c [1]. In this study, As-built specimens were applicable to this equation.

(3) Internal defect
Similarly to (1), the square root of the projected area of the defect at the fatigue crack initiation site is taken as the initial defect dimension √area.

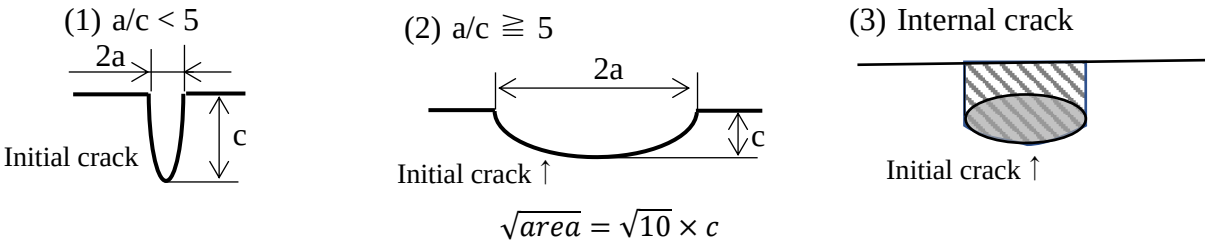

$$\sqrt{area} = \sqrt{10} \times c$$

Fig.5 Schematic models of initial cracks at different types of dimension and locations.

Estimation of ΔK_{th}

The lower limit of fatigue crack growth, ΔK_{th}, was estimated using the initial defect size, √area, and the stress amplitude obtained above. Estimation was based on Ref.[2] and was calculated using equation (1) for surface defects and equation (2) for internal defects.

$$\Delta K = 0.65 \times \Delta\sigma\sqrt{\pi\sqrt{area}} \quad (1)$$

$$\Delta K = 0.5 \times \Delta\sigma\sqrt{\pi\sqrt{area}} \quad (2)$$

The ΔK_{th} of the materials used in this study was estimated based on the graph with ΔK on the vertical axis against the test results.

Crack propagation estimation

Fatigue crack propagation cycles was calculated assuming that the fatigue crack initiated from the defects with the same length of √area determined from fracture surface observations.
The crack propagation cycles were calculated by equation (3) Ref.[3]. The stress intensity factor, ΔK, in the equation, different equations were chosen depending on the specimen shape. The crack shape was assumed to be semicircle and equation of Nishitani et al. Ref.[4], was used. The value estimated by equations (1) and (2) was used for ΔK_{th}.

$$\frac{da}{dN} = C \cdot F \cdot \frac{(\Delta K - \Delta K_{th})^m}{1-\frac{1-\Delta K}{1-RK_C}} = C \cdot \left(\frac{1-f}{1-R}\right)^m \cdot \frac{(\Delta K - \Delta K_{th})^m}{1-\frac{1-\Delta K}{1-RK_C}} \quad (3)$$

The relationship between the number of load cycles and the crack length was calculated on each specimen using equation (3). The number of cycles at which the crack length reached the diameter or thickness of the specimen was regarded as a fatigue fracture cycles and they were compared with the experimental fracture cycles.

Fatigue life estimation

Figure 6 is a comparison of the fatigue test results and the estimated fatigue fracture cycles. Regardless of the size of the defect, the type of defect, or the shape of the specimen, the test results could be estimated by this method with a factor of 2.

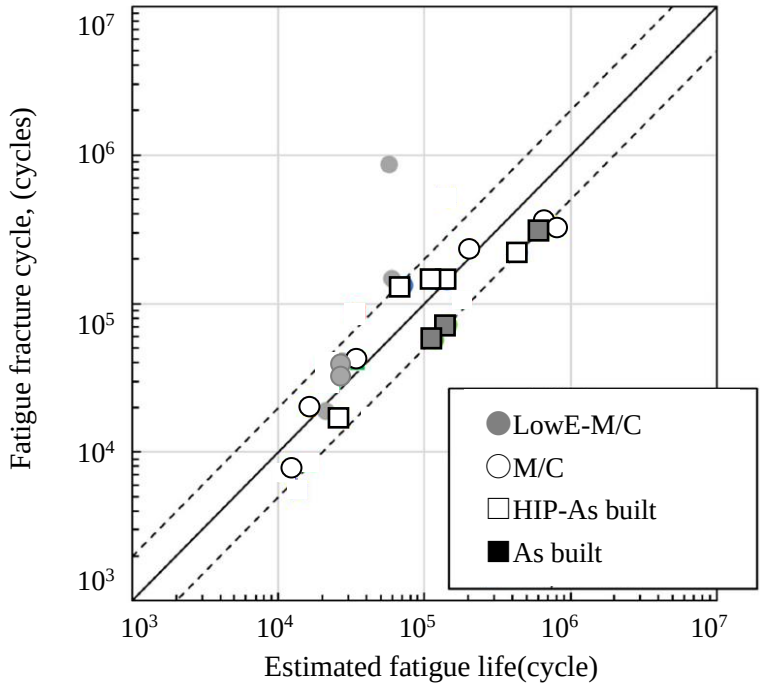

Fig.6 Comparison of estimation result and fatigue test result.

CONCLUSION

In order to quantitatively grasp the effect of internal defects and microstructure through experiments and analysis using linear fracture mechanics in order to clarify the effect of manufacturing process on the fatigue properties of Ti -6 Al -4 V alloy produced by laser powder bed fusion (PBF), fatigue tests were carried out using specimens with different shapes and size of defect and surface morphology, and a method to estimate fatigue life by crack propagation evaluation using the defect dimensions at the fatigue crack initiation sites were examined, and the following results were obtained.
(1) In the fatigue specimens of the same shape, the fatigue strength decreased as the defect size at the crack initiation site increased.
(2) It was confirmed that the fatigue life cycles derived by the fatigue crack growth calculation using the defect size taken from the fracture surface observation results on the machined surface roughly agreed with the experimental results.

REFERENCES

[1] Romano, S. et al., (2018,) *Eng. Frac. Mech.* 187, p.165.
[2] Murakami, Y.et. al., (1988), *Trans. J. Soc. Mech. A*, vol. 54, n. 499, p.413.
[3] Iliopoulos, A. et al., (2018), Aerospace 2018, vol. **5**, p.118.
[4] J. Soc. Mech. Eng., (1987). In: *STRESS INTENSITY FACTORS HANDBOOK*, Vol.2, PERGAMON PRESS.